Exact diagonalization of the Hamiltonian for trapped interacting bosons in lower dimensions

Tor Haugset and Hårek Haugerud

Department of Physics, University of Oslo, P.O. Box 1048 Blindern, N-0316 Oslo, Norway

We consider systems of a small number of interacting bosons confined to harmonic potentials in one and two dimensions. By exact numerical diagonalization of the many-body Hamiltonian we determine the low-lying excitation energies and the ground-state energy and density profile. We discuss the dependence of these quantities on both interaction strength g and particle number N. The ground-state properties are compared to the predictions of the Gross-Pitaevskii equation, and the agreement is surprisingly good even for relatively low particle numbers. We also calculate the specific heat based on the obtained energy spectra. [S1050-2947(98)10504-8]

PACS number(s): 03.75.Fi, 05.30.Jp, 67.40.Db, 32.80.Pj

I. INTRODUCTION

Recent observations of Bose-Einstein condensation in alkali-metal gases confined to harmonic potentials [1,2] has led to an extensive study of the ground-state and low-energy properties of trapped interacting Bose gases. A major part of this work (see, e.g., Refs. [3–9]), presents calculations based on the Bogoliubov approximation or Hartree-Fock theory. Predicted excitation frequencies agree well with experiments [10,11]. The energy spectrum has also been described in terms of a hydrodynamic formalism [12], which agrees with Bogoliubov theory at low energy [8,13]. In the Bogoliubov approximation the system is described in terms of a dominating condensate. Fluctuations induced by finite temperature and interactions are assumed small. At zero temperature, when the effects of excited particles are neglected, the condensate satisfies the Gross-Pitaevskii equation [14–16].

The Bogoliubov approximation is applicable for systems with a large number of particles. In this paper we will, on the contrary, consider systems with relatively few particles, i.e., $N \sim 10$–40. Finite-N effects are then important, and one should in principle use the complete machinery of many-body theory when describing these systems. Here we present the results of such calculations, limiting ourselves to one and two dimensions. The use of such time- and computer-memory-consuming methods puts severe limitations on the size of the system one may describe. On the other hand, it is for such systems the corrections to mean-field calculations are important.

The results presented here are therefore not immediately relevant for the experiments performed with trapped Bose gases so far. Our aim is rather to gain some insight into the effects of the approximations which form the basis of the mean-field theories mentioned above, in the limit of small particle numbers. We are also interested in effects which are specific to one and two dimensions. In addition, future experiments in lower dimensions may explore the range of parameters used here.

The plan of this paper is as follows. In Sec. II we recall the many-body formalism, and describe the steps leading to the diagonalization of the many-body Hamiltonian. The Gross-Pitaevskii approximation, to which we compare our results for the ground state, is discussed in Sec. III. Numeri-

cal results are presented and discussed in Sec. IV. Finally we draw some conclusions in Sec. IV. The Appendix discusses effective couplings in highly anisotropic systems.

II. MANY-BODY DESCRIPTION

As a model for a trapped interacting Bose gas, we study the Hamiltonian density

$$\mathcal{H} = \hat{\Psi}^\dagger(\mathbf{r}) \left[-\frac{\nabla^2}{2m} + V_{\text{ex}}(\mathbf{r}) \right] \hat{\Psi}(\mathbf{r}) + \mathcal{H}_I(\hat{\Psi}^\dagger, \hat{\Psi}), \quad (2.1)$$

where $\hat{\Psi}$ is a bosonic field operator and V_{ex} is the external trapping potential. Units where $\hbar = 1$ are used. We will only consider isotropic harmonic potentials of the form $V_{\text{ex}}(\mathbf{r}) = \frac{1}{2} m \omega^2 r^2$. $\mathcal{H}_I$ describes the interaction. Assuming short-range two-body interaction, this may be written

$$\mathcal{H}_I = g \hat{\Psi}^\dagger \hat{\Psi}^\dagger \hat{\Psi} \hat{\Psi}(\mathbf{r}). \quad (2.2)$$

In the s-wave approximation the coupling constant, or interaction strength g is related to the scattering length a by the equation $g = 2\pi a/m$ in three dimensions. In the Appendix we discuss modifications of this relation in highly anisotropic harmonic traps.

Harmonic modes. As a step toward finding the energy eigenvalues, we expand the field operator in a complete set of modes

$$\hat{\Psi}(\mathbf{r}) = \sum_k \varphi_k(\mathbf{r}) a_k. \quad (2.3)$$

Here a_k annihilates a particle in the state k, and $a_k^\dagger$ creates a particle in the same state. The operators satisfy the commutation relation $[a_k, a_l^\dagger] = \delta_{k,l}$, with other commutators vanishing. In translation-invariant systems it is convenient to choose a set of plane waves. Here we choose to use the harmonic-oscillator eigenfunctions. The Hamiltonian then takes the form

$$H \equiv \int d\mathbf{r} \, \mathcal{H} = \sum_k \omega_k a_k^\dagger a_k + g \sum_{k,l,m,n} f_{klmn} a_k^\dagger a_l^\dagger a_m a_n. \quad (2.4)$$

Here ω_k is the single-particle energy of level k, and f_{klmn} is an overlap integral over four oscillator eigenfunctions:

$$f_{klmn} = \int d\mathbf{r}\ \varphi_k^* \varphi_l^* \varphi_m \varphi_n(\mathbf{r}). \qquad (2.5)$$

Notice that f_{klmn} is symmetric under permutation of the indices. For the complete set of eigenfunctions $\{\varphi_k\}$ we will choose Hermite or Laguerre polynomials for one and two dimensions, respectively. The corresponding overlap integrals can be calculated numerically, though some of them are tabulated [17]. The interaction conserves parity. In one dimension this leads to the constraint $k+l+m+n=$ (even integer) for nonzero f. In two dimensions the rotational symmetry of the external potential suggests the use of radial and angular quantum numbers. The interaction conserves angular momentum, and this again puts a constraint on the possible combinations of creation and annihilation operators.

Many-particle basis and diagonalization. We apply the configuration-interaction approximation and diagonalize the Hamiltonian in a many-particle basis, which in the occupation-number representation may be written in the form

$$|\psi_\alpha\rangle = |n_0 n_1 n_2 \ldots n_K\rangle_\alpha, \qquad (2.6)$$

with α labeling the different distributions of particles. Normalization to unity is assumed. Here n_k is the particle number in the single-particle state k. The particle number is conserved: $\Sigma_k n_k = N$. In a practical calculation we must truncate the basis set at some upper state, here denoted by K. This sets an upper limit for the single-particle energy of the states considered. Such a truncation is, however, somewhat unnatural as far as the many-particle energy is concerned, since it includes the many-particle state $|0_0 \ldots N_K\rangle$ with energy $N\omega_K$, but not the state $|(N-1)_0 \ldots 1_{K+1}\rangle$ which only has energy $\omega_{K+1} + (N-1)\omega_0$. A more consistent way of truncating the basis set is therefore to include only those states which have a total energy up to some maximal value $E_{\max}$. In the actual calculations, $E_{\max}$ will be raised in steps until convergence is reached. The creation operator and annihilation operator act as follows:

$$a_k|n_0 \ldots n_K\rangle = \sqrt{n_k}|n_0 \ldots n_k-1 \ldots n_K\rangle,$$

$$a_k^\dagger|n_0 \ldots n_K\rangle = \sqrt{n_k+1}|n_0 \ldots n_k+1 \ldots n_K\rangle. \qquad (2.7)$$

The number operator is thus $a_k^\dagger a_k$, with eigenvalue n_k.

With a basis set at hand, we may calculate the Hamiltonian matrix elements

$$H_{\alpha',\alpha} = \langle\psi_{\alpha'}|H|\psi_\alpha\rangle = H_{0\alpha}\delta_{\alpha',\alpha} + H_{I\alpha',\alpha}. \qquad (2.8)$$

The free part of the Hamiltonian contributes to the diagonal terms with an amount $\Sigma_k \omega_k n_k$, while the interaction part yields the contribution

$$g \sum_{k,l,m,n} f_{klmn}\langle\psi_{\alpha'}|a_k^\dagger a_l^\dagger a_m a_n|\psi_\alpha\rangle. \qquad (2.9)$$

The symmetries of the interaction can be used to reduce the Hamiltonian matrix to a block-diagonal form. Splitting the complete Fock space into several symmetry-invariant subspaces reduces the dimensions of the Hamiltonian matrix considerably, and enables a numerical diagonalization of much larger systems. In one dimension there are an even- and odd-parity subspaces, and the ground state is a superposition of even-parity states. In two dimensions the subspaces are labeled by the total angular momentum of the many-particle state, and the ground state has zero angular momentum.

The Hamiltonian matrix is relatively sparse, and the iterative Lanczos method [18] is thus well suited for finding the ground state and the lowest excited states. This method enables us to diagonalize much larger matrices than would be possible with standard library routines. However, we use the latter when finding the complete set of energy levels needed for calculating thermodynamic quantities.

Here we would like to emphasize that we have checked the programs thoroughly: They are seen to reproduce well-known results in the case of zero coupling. We have also done some calculations for smaller systems by hand, and find that both the generation of the Hamiltonian matrix and the diagonalization works correctly.

Density profile. Once the Hamiltonian is diagonalized, we have the coefficients for the low lying states, and especially for the ground state. This enables us to find the ground-state density distribution $\rho(\mathbf{r})$. The density operator may be written

$$\hat{n}_\psi = \sum_{k,l} |k\rangle n_{kl}\langle l|, \qquad (2.10)$$

where $|k\rangle$ is a single-particle state, and $n_{kl} = \langle\psi|a_l^\dagger a_k|\psi\rangle$. The density is then $\rho(\mathbf{r}) = \langle\mathbf{r}|\hat{n}_\psi|\mathbf{r}\rangle$. For a state $|\psi\rangle = \Sigma_\alpha C_\alpha|\psi_\alpha\rangle$ this reads

$$\rho(\mathbf{r}) = \sum_{k,l} \varphi_l^* \varphi_k(\mathbf{r}) \sum_{\alpha,\alpha'} C_{\alpha'}^* C_\alpha \langle\psi_{\alpha'}|a_l^\dagger a_k|\psi_\alpha\rangle. \qquad (2.11)$$

Dipole mode. The excitations in this system will in general have interaction-dependent energies. However, as discussed by Fetter and Rokhsar [13], there exists a dipole mode for each spatial dimension of the trap, which corresponds to a harmonic oscillation of the center of mass of the condensate. In Ref. [13] the corresponding raising operator was constructed in the first quantized formalism

$$A_\beta^\dagger = \sum_{i=1}^{N} b_{\beta i}^\dagger, \qquad (2.12)$$

where $b_{\beta i}^\dagger$ is the raising operator for particle number i in dimension β. (We use a different notation than in Ref. [13], in order to avoid confusion with quantities defined here.) With a two-body potential of the form $V(\mathbf{r}_i - \mathbf{r}_j)$ it is easily shown that the excitation energy is ω, i.e., independent of the interaction. Thus for each energy level there must be a ladder of levels with energy spacing ω above. These dipole modes have been found in calculations based on the Bogoliubov approximation [4,7] and in the hydrodynamic description [12]. The occurrence of these states will serve as a check of convergence of the calculated energy levels. For complete-

ness we note that the raising operator in terms of creation and annihilation operators in one dimension takes the form

$$A^\dagger = \sum_k \sqrt{k+1} a_{k+1}^\dagger a_k. \qquad (2.13)$$

Here k labels the Hermite polynomials. Commuting the raising operator with the free-particle Hamiltonian, we find

$$[H_0, A^\dagger] = \omega A^\dagger, \qquad (2.14)$$

and the excitation energy is thus ω. The vanishing of the commutator of $A^\dagger$ with the interaction term is less obvious in this formalism. The commutator becomes

$$[H_I, A^\dagger] = 2g \sum_{k,l,m,n} a_k^\dagger \sqrt{l+1} (f_{kmnl+1} a_n^\dagger a_l$$
$$- f_{kmnl} a_{l+1}^\dagger a_n) a_m, \qquad (2.15)$$

and for each combination $a_k^\dagger a_l^\dagger a_m a_n$ the prefactor vanishes. This is due to the following relation between the overlap integrals:

$$\sqrt{d+1} f_{abcd+1} + \sqrt{c+1} f_{abc+1d} = \sqrt{a} f_{a-1bcd} + \sqrt{b} f_{ab-1cd}. \qquad (2.16)$$

Breathing mode. In two dimensions the many-body Hamiltonian has an $SO(2,1)$-symmetry discovered by Pitaevskii and Rosch [19]. This symmetry gives rise to excitations of energy 2ω identified with the breathing mode of the condensate. The excitation spectra for the planar systems must therefore contain ladders both with energy spacing ω and 2ω. The symmetry is broken when a UV energy cutoff is introduced in the system. Such a cutoff is inherent in our calculation. We therefore expect that the level spacing 2ω will be less accurate than the spacing ω caused by the dipole excitations.

III. MEAN-FIELD APPROXIMATION

One of the purposes of this paper is to compare the predictions of the many-body calculation with those of mean-field theory for quantities such as the ground-state energy and density distribution. The condensate is in the Gross-Pitaevskii (GP) approximation [14,15] described by a classical, macroscopic Bose field governed by the Hamiltonian density per particle

$$\mathcal{H}_{cl}/N = \Phi^*(\mathbf{r})\left(-\frac{\nabla^2}{2m} + V_{ex}(\mathbf{r})\right)\Phi(\mathbf{r}) + gN[\Phi^*\Phi(\mathbf{r})]^2. \qquad (3.1)$$

The field is rescaled here to satisfy $\int d\mathbf{r}\Phi^*\Phi = 1$, thus the factor N in front of the interaction term. Notice that the coupling g and the particle number N occur only in the combination gN, as opposed to the many-body description. Minimalization of the corresponding Hamiltonian $H_{cl} = \int d\mathbf{r}\mathcal{H}_{cl}$ leads to the nonlinear Schrödinger (or Gross-Pitaevskii) equation

$$\left(-\frac{\nabla^2}{2m} + V_{ex}(\mathbf{r}) - \mu\right)\Phi(\mathbf{r}) + 2gN\Phi^*\Phi\Phi(\mathbf{r}) = 0. \qquad (3.2)$$

The chemical potential introduced is given by the normalization of Φ. This equation can be derived from the Hartree-Fock-Bogoliubov approximation when the effect of excited particles is neglected [16].

Oscillator basis. The equation for Φ may be solved introducing a harmonic-oscillator basis

$$\Phi(\mathbf{r}) = \sum_k c_k \phi_k(\mathbf{r}). \qquad (3.3)$$

Normalization now corresponds to $\Sigma_k|c_k|^2 = 1$. The equation then takes the form

$$\sum_k (\omega_k - \mu)c_k\phi_k(\mathbf{r}) + 2gN\sum_{k,l,m} c_k^* c_l c_m \phi_k^* \phi_l \phi_m(\mathbf{r}) = 0. \qquad (3.4)$$

Multiplying with ϕ_n^* and integrating, we finally end up with the set of equations

$$(\omega_n - \mu)c_n + 2gN\sum_{k,l,m} c_k^* c_l c_m f_{klmn} = 0, \qquad (3.5)$$

where f again is the overlap integral over four harmonic-oscillator eigenfunctions. The basis set is truncated at some level K, and K is raised until convergence is reached. The corresponding finite set of equations may be solved by use of the Newton-Raphson method. This method was applied in Ref. [7] for the case of a three-dimensional Bose gas. Solutions in one dimension have also been obtained earlier [6]. Again the symmetry of the ground state may be used to choose the proper subset of eigenfunctions. In one dimension we only have to consider even functions. In two dimensions only zero angular momentum eigenfunctions contribute.

Once the coefficients c_k are determined, one must check if the normalization condition is satisfied. If not, a different chemical potential is chosen, and the process is repeated until normalization is obtained. Having the correct coefficients, we easily find the ground-state density profile

$$\rho(\mathbf{r}) = \left|\sum_k c_k \phi_k(\mathbf{r})\right|^2. \qquad (3.6)$$

In addition, the ground-state energy per particle reads

$$\sum_k \omega_k |c_k|^2 + gN\sum_{klmn} c_k^* c_l^* c_m c_n f_{klmn}. \qquad (3.7)$$

IV. NUMERICAL RESULTS

In the following we present the results of the numerical diagonalization of the many-body Hamiltonian. In one dimension we have truncated the many-body basis at a cutoff energy $E_{max} = 38\,\omega$. This corresponds to a basis with blocks of up to 80 524 many-body states. In two dimensions the number of overlap integrals for a given E_{max} is considerably higher than in one dimension. Moreover, the generation of
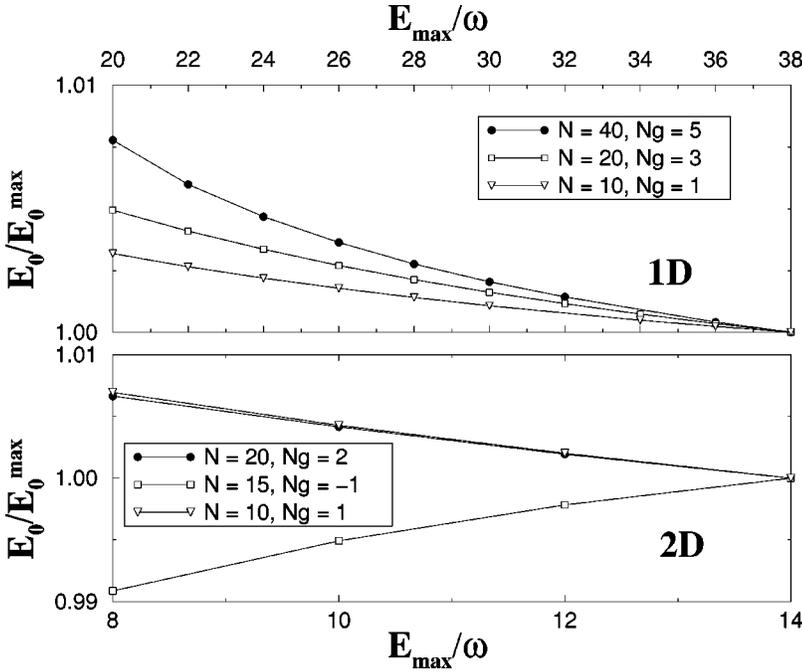
FIG. 1. Convergence of the ground-state energy. We plot the ratio of the ground-state energy E_0 for the given cutoff E_{max} and the energy E_0^{max} found using the highest E_{max}. The upper graph is for one dimension, and the lower for two dimensions.

matrix elements turns out to be very time consuming. We have therefore stopped at $E_{max} = 14\,\omega$, with a basis with blocks of up to 4532 states in two dimensions. Energies are measured in units of the oscillator frequency and lengths in units of the typical oscillator width $1/\sqrt{m\omega}$. g refers to the corresponding dimensionless interaction strength ($\tilde{g}_{1D}, \tilde{g}_{2D}$) as obtained in the Appendix.

In Fig. 1 we show the ground-state energy as function of the cutoff energy E_{max}. The plotted quantity is the ratio of the ground-state energy for the given E_{max} and the energy found using the highest E_{max} considered. The upper graph is for one dimension, and the lower for two dimensions. In one dimension, the relative difference in ground-state energy going from $36\,\omega$ to $38\,\omega$ is seen to be about 0.05% or less. Going from $12\,\omega$ to $14\,\omega$ in two dimensions, the shift is about 0.2%. The convergence of the excitation energies is found to be considerably faster for the lowest levels, but is slower at high energy. This will be seen below in the deviation of the interaction-independent energies from the exact values $n\omega$.

A. Ground-state energy

In this subsection we show the effect of the interaction on the energy of the ground state. In all figures the ideal gas ground-state energy is set to zero.

Linear Bose gas. Figure 2 shows the ground-state energy in one dimension, both in the many-body description and in the Gross-Pitaevskii approximation. For a given Ng the energy resulting from the many-body calculation is seen to converge toward the mean-field value as the particle number N is increased. The discrepancy between the approximations increases with Ng.

The discrepancies found between the two approximations might to some extent be removed by the introduction of an effective coupling constant in the mean-field theory. For a set of couplings g_0 and particle numbers N, we find the rescaled coupling which in the GP approximation yields the

corresponding energy given by the many-body calculation. In Fig. 3 this rescaled coupling multiplied by N is plotted (filled circles) as a function of $1/N$ for various values of the bare coupling. The corresponding value of Ng_0 is found at $1/N = 0$. For the range of parameters considered, the lines look very linear. Below, we compare these results with the effective coupling based on calculations of the core density in the ground state.

Planar Bose gas. The insert in Fig. 4 shows the Gross-Pitaevskii ground-state energy in two dimensions as function of Ng. The energy falls rapidly with decreasing, negative coupling. With a basis of up to 28 oscillator eigenfunctions, we have not been able to reach convergence near $E_0/N = -\omega$. It seems though that $dE_0/d(Ng)$ approaches infinity as we get closer to this point, thus indicating that no stable
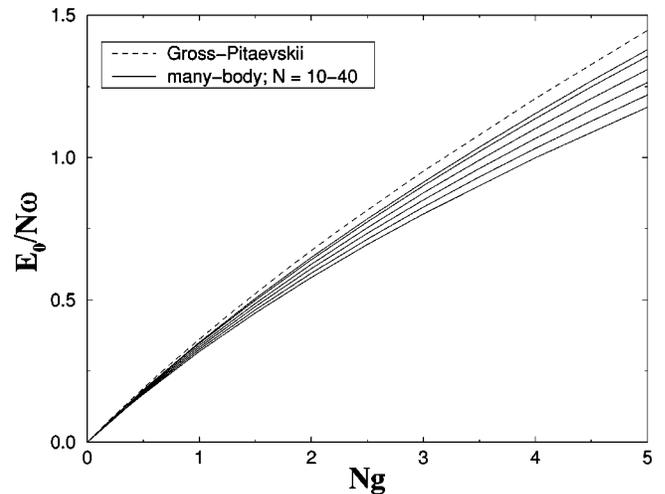

FIG. 2. Ground-state energy E_0 per particle in one dimension measured in units of ω as a function of interaction strength g for particle numbers $N = 10,\ 12,\ 15,\ 20,\ 30,$ and 40, starting from below. The results of the many-body calculation converge toward the mean-field result as the particle number increases.
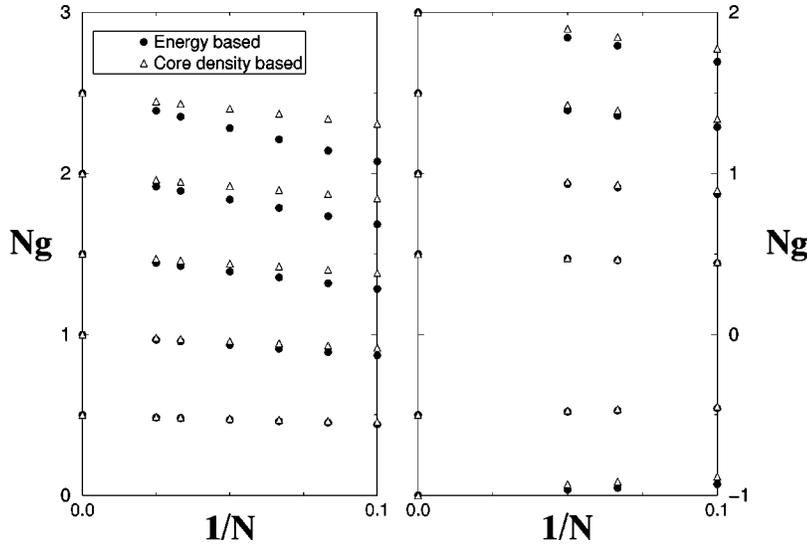
FIG. 3. Effective coupling Ng in one (left) and two (right) dimensions. The corresponding values of Ng_0 are found at $1/N = 0$. Effective couplings based on the energy and the core density of the ground state are compared.

ground state may be formed for stronger attractive couplings. This is agreement with Pitaevskii's analysis of the system [20], where it is shown that an attractive interaction leads to collapse of the gas for energies more than ω below the ideal gas ground-state energy. Similar conclusions are drawn in Ref. [21].

The Gross-Pitaevskii ground state energy is in Fig. 4 also plotted together with the results of the many-body calculation for $N = 10,\ 15,$ and 20. The mean-field approximation is approached as N increases. We have calculated the effective coupling Ng which, used in the GP approximation, reproduces the energy obtained in the many-body calculation. This effective coupling is plotted as filled circles in the right graph of Fig. 3. The results are all for the highest cutoff energy $E_{max} = 14\omega$. We again find that Ng depends nearly linearly on $1/N$.

B. Excitations

In Sec. II we saw that the excitation energies must consist of ladders with energy spacing ω. This is due to the existence of the collective raising operator $A^\dagger$. In two dimensions, the breathing mode leads to additional ladders with spacing 2ω. The bottom of each of the ladders must, however, be determined by other means, and here we present the results of the numerical diagonalization of the many-body Hamiltonian.

Linear Bose gas. In Fig. 5, the lowest excitation energies in one dimension are given as functions of Ng for the case of 30 particles. The degeneracy at zero coupling is split by the interaction. For each level in the ideal case, one level remains independent of the coupling. These levels correspond to excitations described by $A^\dagger$ from the ground state. The others spread out below, and above each of these we find the mentioned ladder of levels. Similar results are obtained for $N = 10,\ 12,\ 15,\ 20,$ and 40. The relative shift in the energies going from $N = 10$–40 with a given Ng is less than 1% for the range of parameters presented in Fig. 5.

The splitting of the degeneracy by the interaction leads to a more even distribution of energy levels than in the free case. As an illustration of this, Fig. 6 shows the number of energy levels $n_{1D}(E)$ (right curves) below a given energy E measured from the ground state. We have taken $N = 20$, and

the coupling ranges from $Ng = 0$–2 in steps of 0.2. This summed density of states is indeed smoothed by the presence of the interaction. Note that the curves coincide at points $(E - E_0)/\omega = n$. This happens because all interaction-dependent excitation energies lie in the gap below the corresponding undisturbed level for the considered values of the coupling.

Planar Bose gas. The lowest energy levels of a planar system with 20 bosons are given in Fig. 7 as function of the dimensionless coupling. For each level with nonzero angular momentum L, there is a level with the same energy and angular momentum $-L$. The degeneracy at $g = 0$ is partially lifted for nonzero g, but again there are levels which are unaffected by the interaction. These are reached by the two dipole excitations and the breathing mode excitation from the ground state. The modes also give rise to a set of ladders above the interaction-dependent levels. Since the energies of all three interaction-independent modes are multiples of ω,
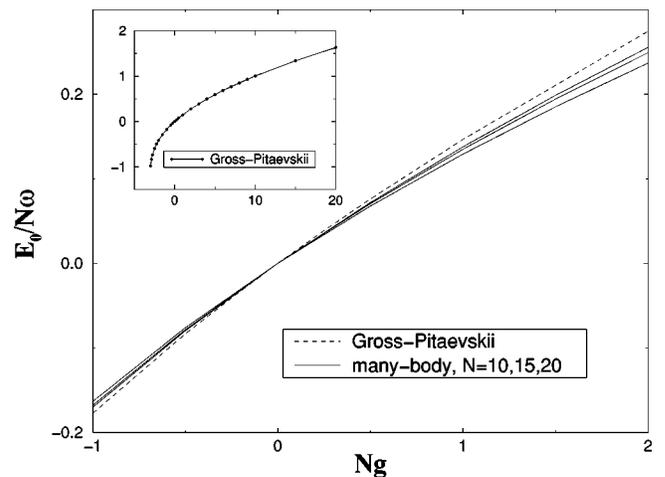

FIG. 4. Ground-state energy E_0 per particle in two dimensions measured in units of ω as a function of interaction strength g for particle numbers $N = 10,\ 15,$ and 20 starting from below. The results of the many-body calculation are compared to the mean-field approximation (Gross-Pitaevskii), which is approached as the particle number increases. The inset shows the energy in the mean-field approximation over a broader range of the interaction strength.
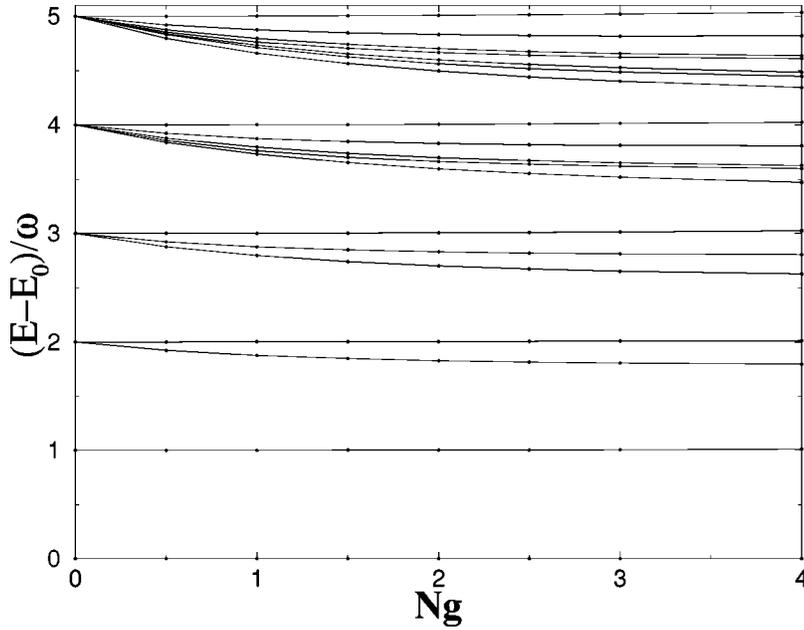
FIG. 5. Excitation energies $(E-E_0)/\omega$ in a one-dimensional system of 30 bosons as a function of the interaction strength g.

there is a high degree of degeneracy even for $g \neq 0$ in this system.

In Fig. 6 the corresponding summed density of states $n_{2D}(E)$ (left curves) is plotted for 15 bosons with the coupling running from $Ng = -1$ to 2 in steps of 0.5. Levels for both positive and negative angular momentum are included. The steplike form of the curve for the free case is again smoothed by the interaction.

For stronger couplings we do not quite reproduce the independence of the interaction. This is due to the truncation of the basis of states. However, since we know that these levels must approach $(E-E_0)/\omega =$ integer as the basis set is increased, the deviation gives a good indication of the accuracy of the results. In two dimensions we find that the convergence is better for those levels involving only dipole excitations than for those which are reached (partly) by the
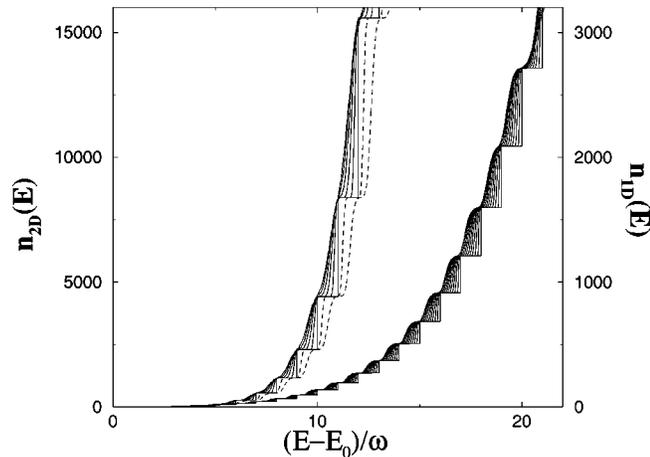
breathing mode. As discussed above, this is an expected effect of the existence of the energy cutoff.

C. Ground-state density

The ground state can, in the GP approximation, be written as a superposition of oscillator functions with even parity or zero angular momentum in one and two dimensions, respectively. In the many-body description this is no longer true, and single-particle states with other quantum numbers will contribute. We here show how this affects the ground-state density.

For large gN the interaction energy dominates the kinetic energy, and one may neglect the kinetic term in the GP equation. This is the Thomas-Fermi (TF) approximation [3]. The solution is now simply

$$|\Phi(\mathbf{r})|^2 = \frac{1}{2gN}[\mu - V_{ex}(\mathbf{r})]\theta[\mu - V_{ex}(\mathbf{r})]$$

FIG. 6. Summed density of states in one- (right curves, n_{1D}) and two-dimensional (left curves, n_{2D}) systems of 20 and 15 bosons, respectively. The interaction strength is in the range $Ng = 0, 0.2, \ldots, 2$ in one dimension, and $Ng = -1, -0.5, \ldots, 2.5$ in two dimensions. Ng increases from right to left, and negative interaction strengths are indicated by dashed lines.
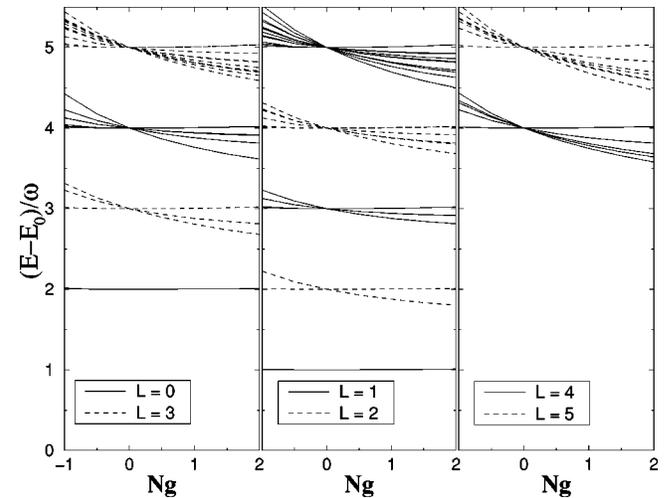

FIG. 7. Excitation energies $(E-E_0)/\omega$ in a two-dimensional system of 20 bosons as a function of the interaction strength. L is the angular momentum.
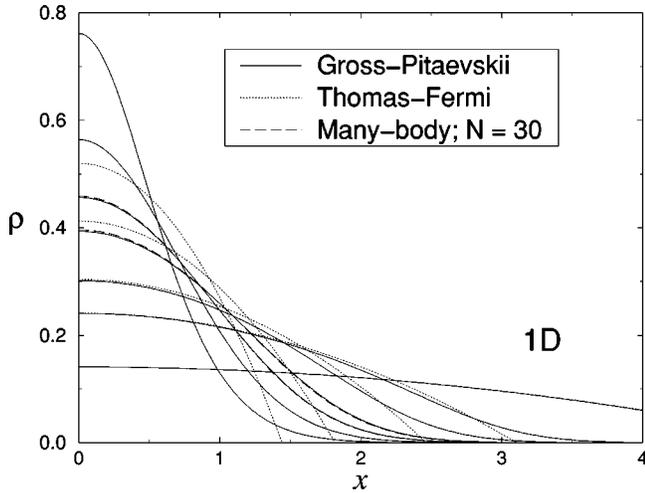
FIG. 8. Normalized ground-state density ρ in one dimension. The density is plotted as a function of the dimensionless radius $x = r\sqrt{m\omega}$. The solid curves give the density in the Gross-Pitaevskii approximation for $Ng = -1$, 0, 1, 2, 5, 10, and 50. The dotted curves show the result of the Thomas-Fermi approximation for repulsive interaction. The density obtained in the exact many-body calculation with 30 particles is shown as dashed lines for $Ng = 1$ and 2.

$$\equiv \frac{m\omega^2}{4gN}(R^2 - r^2)\,\theta(R^2 - r^2). \qquad (4.1)$$

This describes a condensate density which vanishes outside the radius $R = \sqrt{2\mu/m\omega^2}$. Here we compare the normalized density ρ in the TF approximation with the exact solution of the Gross-Pitaevskii approximation, and also with the full many-body calculation. The TF approximation in three dimensions was studied earlier in Ref. [5].

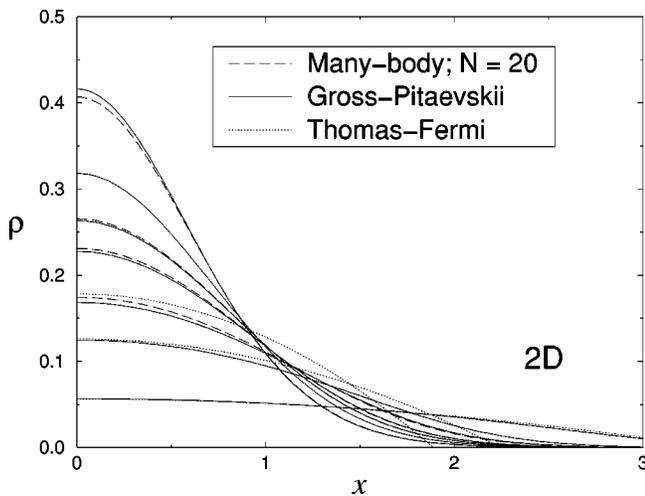In Figs. 8 and 9 we plot the normalized ground-state den-

FIG. 9. Normalized ground-state density ρ in two dimensions. The density is plotted as a function of the dimensionless radius $x = r\sqrt{m\omega}$. The solid curves give the density in the Gross-Pitaevskii approximation for $Ng = -1$, 0, 1,2, 5, 10, and 50. The dotted curves show the result of the Thomas-Fermi approximation for repulsive interaction $Ng = 5$, 10, and 50. The density obtained in the exact many-body calculation with 20 particles is shown as dashed lines for $Ng \leqslant 5$.

sity $\rho(x)$ as a function of the dimensionless radius $x = r\sqrt{m\omega}$ in one and two dimensions, respectively. The Thomas-Fermi approximation is seen to reproduce the core density $\rho(x = 0)$ for interaction strengths above $Ng \sim 5$ in one dimension, and above $Ng \sim 10$ in two dimensions. The approximation gets worse as the distance from the core is increased, where the density has a sharp cutoff in the Thomas-Fermi approximation. For the lowest values of the interaction strength we compare the Gross-Pitaevskii approximation to the full many-body calculation with $N = 30$ and 20 in one and two dimensions, respectively. The GP approximation yields quite good results, especially at large distances, but it tends to overestimate the effect of the interaction. Still, the mean-field theory seems to work better for the density than for the ground-state energy.

We may again try to compensate for the deviation by introducing an effective interaction strength, as done for the energy calculations. The corresponding values of Ng are shown as triangles in Fig. 3. The one- and two-dimensional results are for $E_{max}/\omega = 38$ and 14, respectively.

The effective couplings are different from those based on the energy calculation, and the relative difference increases with Ng_0. The agreement is however quite good for $Ng_0 = 0.5$ and 1 in two dimensions. But, in general, a simple rescaling of the interaction cannot account for all many-body effects in the ground state.

D. Specific heat

Having obtained the lowest excitation energies of the system of trapped bosons, it is straightforward to find the partition function and the thermodynamical quantities one may derive thereof. The validity of these results is limited to low temperatures $T \ll E_{max}$. Just how low the temperature must be will be clear in the examples which follow.

Let us first consider the one-dimensional system. With 20 particles and a cutoff at $E_{max} = 26\,\omega$, we find the specific heat plotted in the left graph of Fig. 10. The coupling ranges from $Ng = 0$ to 2 in steps of 0.5, starting from below at low temperatures. The dotted line is the specific heat for 20 non-interacting bosons calculated in the canonical ensemble. We also show the result of a calculation in the grand-canonical ensemble. For particle numbers as low as this, the two ensembles predict somewhat different specific heats. The exact curve agrees with the curve for $g = 0$ up to a temperature around 1.5ω. At higher temperatures the many-body calculation breaks down. For temperatures where the results are valid, we find that the repulsive interaction yields a higher specific heat than in the case of noninteracting particles. This happens because the interaction brings most of the energy levels closer to the ground state. The effect of the interaction grows with increasing temperature in this regime.

We have also calculated the specific heat for a two-dimensional system of 15 bosons. The cutoff here is $E_{max} = 14\omega$, and the basis thus contains states with angular momentum up to $L = \pm 14$. The specific heat is shown in the right graph of Fig. 10. The calculation now breaks down around $T/\omega = 1$. For comparison we have included the specific heat of 15 noninteracting bosons as given in the grand-canonical ensemble. Again, a repulsive interaction increases the specific heat, while it is decreased in the attractive case.
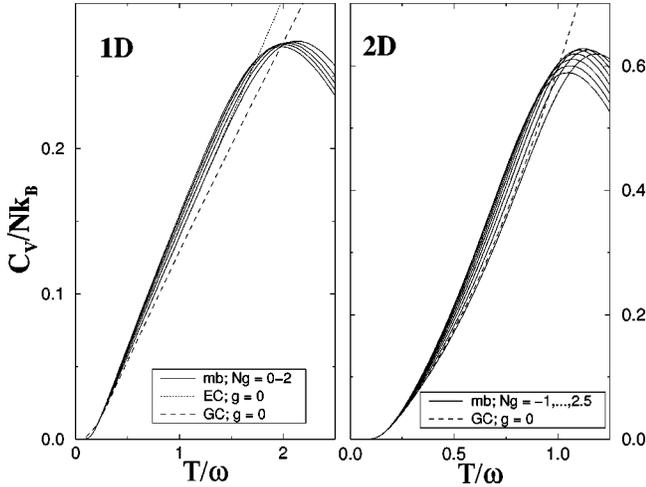
FIG. 10. Specific heat C_V per particle measured in units of k_B for one- (left) and two-dimensional (right) systems of 20 and 15 bosons, respectively. The specific heat is plotted as function of the reduced temperature T/ω. In one dimension the interaction strength runs from $Ng = 0$ to 2 and in two dimensions from -1 to 2.5. Ng increases from below in steps of 0.5. The many-body results (mb) are compared to the curve for the ideal gas as given in the grand canonical ensemble (GC). In one dimension we also show the exact result for the ideal gas in the canonical ensemble (EC). Notice the breakdown at higher temperatures due to the cutoff in the energy spectra.

There is no Bose-Einstein condensation for an ideal, *homogeneous* gas in two dimensions. In the presence of a harmonic trapping potential, condensation may, however, occur [22,23]. The condensation temperature $T_0 = \hbar\omega\sqrt{N/\zeta(2)}$ persists in the thermodynamic limit, which is found by taking $N \to \infty, \omega \to 0$ while keeping the average particle density $\rho \sim N\omega^2$ constant. Recently, Mullin [24] studied a two-dimensional system with attractive interaction in the thermodynamic limit. He found that the normal state has a transition temperature $T < T_0$, but *not* to a Bose condensed phase. This agrees with the earlier findings of Shevchenko [22]. Keeping, instead N and ω finite, one should find a *non-zero* temperature at which condensation sets in. Although one might study this by the method used here, we cannot derive any decisive results as far as the condensation temperature is concerned. For this one would need excitation energies going considerably higher than what we have considered.

V. DISCUSSION AND CONCLUSION

In this paper we have presented results of calculations in the configuration-interaction approximation on systems with 10–40 interacting bosons confined to harmonic traps in one and two dimensions. By use of a set of many-body states and decomposition of the fields in harmonic modes, we have diagonalized the Hamiltonian numerically. The resulting ground-state properties have been compared to the predictions of the Gross-Pitaevskii equation. The largest difference is found for the ground-state energy, while for the ground-state density the mean-field predictions are considerably more accurate, at least for larger Ng.

We have tried to compensate by introducing an effective interaction strength in the mean-field description. This has

been done by computing that interaction strength which, when applied in the Gross-Pitaevskii equation, yields the same ground-state energy and core density as found in the full many-body calculation. In two dimensions, and for $Ng_0 = 0.5$ and 1 the effective couplings obtained from matching energy and from matching core density agree quite well. But, in general, rescaling based on ground-state energy and core density result in different effective couplings. Thus this simple rescaling cannot account for all many-body effects in the ground state.

We have also considered the lowest excitation energies. In both one and two dimensions we have reproduced the interaction independent levels which must be present in these systems [13,19]. The interaction breaks the degeneracy in the noninteracting gas completely in one dimension. In two dimensions the two dipole modes and the breathing mode assure a high degree of degeneracy even for nonzero interaction. We have calculated the specific heat based on these excitation energies. For low temperatures, where the results are valid, the repulsive interaction increases the specific heat, while it is decreased in the attractive case.

It would be interesting to compare the obtained excitation energies with the results of calculations based on the Bogoliubov or Hartree-Fock approximations. One might also use the obtained density of states as a basis for calculations in the microcanonical ensemble. Finally, the parameter range might be extended by choosing a more suitable basis of single-particle states, such as the Hartree-Fock states.

APPENDIX A: EFFECTIVE COUPLING IN LOWER DIMENSIONS

Inspired by proposed experiments in lower dimensions [25,26], here we will here consider the effect of having a strongly anisotropic trapping potential. Assuming $\omega_z \ll \omega_{x,y}$ or $\omega_z \gg \omega_{x,y}$ the system should effectively be one or two dimensional. When the larger oscillator energy dominates all other energies in the system, we may assume that there will be no excitations in this direction. This means that the field operator may be written as

$$\hat{\Psi}(x,y,z) = \sum_k \phi_0(x)\phi_0(y)\phi_k(z)a_{00k} \qquad (A1)$$

for the one-dimensional case, and

$$\hat{\Psi}(x,y,z) = \sum_k \phi_0(z)\phi_k(x,y)a_{0k} \qquad (A2)$$

for the two-dimensional case. We may then integrate over the spatial variables corresponding to the stronger oscillation frequencies. This results in a rescaling of the coupling constant g in Eq. (2.2):

$$g_{2D} = g_{3D} \sqrt{\frac{m\omega_z}{2\pi}} \quad \text{and} \quad g_{1D} = g_{3D} \frac{m\omega_{xy}}{2}. \quad (A3)$$

Measuring energy in units of the remaining oscillator frequency ω and lengths in units of the oscillator length $1/\sqrt{m\omega}$, we obtain the dimensionless coupling constants

$$\widetilde{g}_{2D} = \sqrt{2\pi} \frac{a}{a_z} \quad \text{and} \quad \widetilde{g}_{1D} = \pi \sqrt{\frac{\omega_{xy}}{\omega_z}} \frac{a}{a_{xy}}, \quad (A4)$$

where $a_i = \sqrt{\hbar/m\omega_i}$ and $a = mg_{3D}/2\pi\hbar^2$. Here we have reintroduced $\hbar$. The effective coupling is seen to increase with the strength of the stronger oscillator frequency. This is an effect of reducing the length in which the particle density may extend in the dimensions integrated out.

As an example of a possible physical realization, we mention that Ketterle and van Druten [25] have suggested an experiment with $\omega_z/\omega_{xy} \sim 10^{-3}$ and $\omega_{xy} \sim 200$ nK. With a scattering length of typically 100 Bohr radii, this yields an effective one-dimensional coupling $\widetilde{g}_{1D} \sim 1$. This corresponds to a strong-coupling system for any finite number of particles. Other configurations may yield a weaker effective coupling.

[1] K. B. Davis, M.-O. Mewes, M. R. Andrews, N. J. van Druten, D. S. Durfee, D. M. Kurn, and W. Ketterle, Phys. Rev. Lett. **75**, 3969 (1995).

[2] M. H. Anderson, J. R. Ensher, M. R. Matthews, C. E. Wieman, and E. A. Cornell, Science **269**, 198 (1995).

[3] G. Baym and C. Pethick, Phys. Rev. Lett. **76**, 6 (1996).

[4] K. G. Singh and D. S. Rokhsar, Phys. Rev. Lett. **77**, 1667 (1996).

[5] M. Edwards *et al.*, Phys. Rev. A **53**, R1950 (1996).

[6] P. A. Ruprecht, M. J. Holland, K. Burnett and M. Edwards, Phys. Rev. A **51**, 4704 (1995).

[7] M. Edwards *et al.*, Phys. Rev. Lett. **77**, 1671 (1996).

[8] F. Dalfovo *et al.*, Phys. Rev. A **56**, 3840 (1997).

[9] B. D. Esry, Phys. Rev. A **55**, 1147 (1997).

[10] D. S. Jin, *et al.*, Phys. Rev. Lett. **77**, 420 (1996).

[11] M.-O. Mewes *et al.*, Phys. Rev. Lett. **77**, 988 (1996).

[12] S. Stringari, Phys. Rev. Lett. **77**, 2360 (1996).

[13] A. L. Fetter and D. S. Rokhsar, Phys. Rev. A **57**, 1191 (1998).

[14] E. P. Gross, Nuovo Cimento **20**, 454 (1961); J. Math. Phys. **4**, 195 (1963).

[15] L. P. Pitaevskii, Zh. Éksp. Teor. Fiz. **40**, 646 (1961) [Sov. Phys. JETP **13**, 451 (1961)].

[16] A. Griffin, Phys. Rev. B **53**, 9341 (1996).

[17] I. S. Gradshteyn and I. M. Rhyzhik, *Table of Integrals, Series and Products* (Academic, New York, 1965).

[18] C. Lanczos, J. Res. Natl. Bur. Stand. **45**, 255 (1950).

[19] L. P. Pitaevskii and A. Rosch, Phys. Rev. A **55**, R 853 (1997).

[20] L. P. Pitaevskii, Phys. Lett. A **221**, 14 (1996).

[21] K. Watanabe, T. Mukai and T. Mukai, Phys. Rev. A **55**, 3639 (1997).

[22] S. I. Shevchenko, Zh. Éksp. Teor. Fiz. **100**, 1824 (1991) [Sov. Phys. JETP **73**, 1009 (1991)].

[23] W. J. Mullin, J. Low Temp. Phys. **106**, 615 (1997).

[24] W. J. Mullin, e-print cond-mat/9709077.

[25] W. Ketterle and N. J. van Druten, Phys. Rev. A **54**, 656 (1996).

[26] T. Pfau and J. Mlynek, *Bose-Einstein Condensation*, OSA Trends in Optics and Photonic Series Vol. 7 (Optical Society of America, Washington, DC, 1997), p. 33.